The Heteronuclear Cluster Chemistry of the Group 1B Metals. Part 4.[1] Synthesis, Structures, and Dynamic Behaviour of Group 1B Metal–Ruthenium Cluster Compounds containing Sulphur Ligands. *X*-Ray Crystal Structures of $[M_2Ru_3(\mu_3\text{-}S)(\mu\text{-}Ph_2PCH_2PPh_2)(CO)_9]$ (M = Cu or Au)†

Scott S. D. Brown, Stephen Hudson, and Ian D. Salter*
Department of Chemistry, University of Exeter, Exeter EX4 4QD
Mary McPartlin*
School of Chemistry, The Polytechnic of North London, London N7 8DB

Treatment of a tetrahydrofuran solution of the salt $K_2[Ru_3(\mu_3\text{-}S)(CO)_9]$ with the complex $[MX(PPh_3)]$ (M = Cu or Au, X = Cl; M = Ag, X = I), in the presence of $TlPF_6$, affords a mixture of cluster compounds, $[MRu_3(\mu\text{-}H)(\mu_3\text{-}S)(CO)_9(PPh_3)]$ [for M = Cu (**2**), Ag (**3**), or Au (**4**)], $[MRu_3(\mu\text{-}H)(\mu_3\text{-}S)(CO)_8(PPh_3)_2]$ [for M = Cu (**5**) or Ag (**6**)], and $[M_2Ru_3(\mu_3\text{-}S)(CO)_9(PPh_3)_2]$ [for M = Cu (**8**), Ag (**9**), or Au (**10**)]. In addition, the pentanuclear clusters $[M_2Ru_3(\mu_3\text{-}S)(\mu\text{-}Ph_2PCH_2PPh_2)(CO)_9]$ [M = Cu (**12**) or Au (**13**)] can be synthesized from the reaction between $K_2[Ru_3(\mu_3\text{-}S)(CO)_9]$ and $[M_2(\mu\text{-}Ph_2PCH_2PPh_2)Cl_2]$, using $TlPF_6$. Infrared and n.m.r. spectroscopic data imply that the tetranuclear copper- or silver-containing species (**2**), (**3**), (**5**), and (**6**) all adopt the same 'butterfly' MRu_3 metal-core geometry as that previously established for the Au cluster (**4**) and that the pentanuclear Cu and Ag species (**8**) and (**9**) exhibit the same trigonal-bipyramidal M_2Ru_3 framework as that determined for the Au cluster (**10**). However, *X*-ray diffraction studies on the bidentate phosphine-containing pentanuclear Cu_2Ru_3 species (**12**) and its Au_2Ru_3 analogue (**13**) reveal two different metal-core structures. The Cu cluster (**12**) has a trigonal-bipyramidal metal skeleton [Cu–Cu 2.515(3), Cu–Ru 2.552(2)—2.794(2), Ru–Ru 2.814(2)—2.856(2) Å], with one of the two phosphine-bridged Cu atoms occupying an equatorial site and the other an axial site. The S atom caps the Ru_3 face of the trigonal-bipyramidal unit. In the Au species (**13**), the metal framework structure is intermediate between a trigonal bipyramid and a square-based pyramid [Au–Au 2.802(1), Au–Ru 2.742(1)—2.836(1), Ru–Ru 2.773(2)—2.968(2) Å]. Variable-temperature n.m.r. studies show that, at ambient temperature in solution, the coinage metals in each of the pentanuclear clusters (**8**)—(**10**), (**12**), and (**13**) are exchanging between the two distinct sites in the cluster skeleton, the PPh_3 groups in the copper–ruthenium species (**2**) and the silver–ruthenium species (**3**), (**6**), and (**9**) are undergoing intermolecular exchange between clusters, and the CO ligands in all of the clusters exhibit dynamic behaviour involving intramolecular site-exchange.

The first paper in this series[2] describes our interest in experimentally comparing the structures and chemical properties of heteronuclear clusters containing $M(PR_3)$ (M = Cu or Ag, R = alkyl or aryl) fragments with those of the analogous gold-containing species. It has been previously reported[3] that the reaction between $[Ru_3(\mu\text{-}H)_2(\mu_3\text{-}S)(CO)_9]$ and $[AuMe(PPh_3)]$ affords a mixture of cluster compounds, $[Ru_3(\mu\text{-}H)_2(\mu_3\text{-}S)(CO)_7(PPh_3)L]$, $[AuRu_3(\mu\text{-}H)(\mu_3\text{-}S)(CO)_8(PPh_3)L]$, and $[Au_2Ru_3(\mu_3\text{-}S)(CO)_8(PPh_3)_2L]$ (L = CO or PPh_3). A trigonal-bipyramidal metal skeleton, with one gold atom occupying an equatorial site and the other an axial site, was established for $[Au_2Ru_3(\mu_3\text{-}S)(CO)_8(PPh_3)_3]$ by *X*-ray diffraction.[3] From i.r. and n.m.r. spectroscopic data, it was concluded[3] that the closely related species $[Au_2Ru_3(\mu_3\text{-}S)(CO)_9(PPh_3)_2]$ also adopts this core geometry and that the tetranuclear clusters $[AuRu_3(\mu\text{-}H)(\mu_3\text{-}S)(CO)_8(PPh_3)L]$ both exhibit a 'butterfly' metal framework, with the gold atom occupying a 'wing-tip' site. These structural conclusions were subsequently confirmed by *X*-ray diffraction studies[4] on the Au_2Ru_3 species and on $[AuRu_3(\mu\text{-}H)(\mu_3\text{-}S)(CO)_9(PPh_3)]$. Furthermore, variable-temperature $^{31}P\text{-}\{^1H\}$ n.m.r. studies showed[3] that, in solution, both of the pentanuclear clusters $[Au_2Ru_3(\mu_3\text{-}S)(CO)_8(PPh_3)_2L]$ undergo dynamic behaviour involving an exchange of the gold atoms between the two distinct sites in the cluster skeletons and that this process still occurs at −90 °C. In view of the novel fluxional properties of these pentanuclear gold–ruthenium species, we have extended this work to the synthesis of the analogous copper and silver clusters. We also report how the structures and dynamic behaviour of this type of cluster are affected when the two coinage metals are linked together by the bidentate phosphine $Ph_2PCH_2PPh_2$.

Results and Discussion

Treatment of a tetrahydrofuran (thf) solution of $[Ru_3(\mu\text{-}H)_2(\mu_3\text{-}S)(CO)_9]$ with an excess of KH or an ethanol solution of the cluster with an excess of KOH removes the two hydrido ligands to give the salt $K_2[Ru_3(\mu_3\text{-}S)(CO)_9]$. A subsequent metathesis reaction with $[N(PPh_3)_2]Cl$ yields (82%) the ruthenium cluster dianion as its yellow $[N(PPh_3)_2]^+$ salt, $[N(PPh_3)_2]_2[Ru_3(\mu_3\text{-}S)(CO)_9]$ (**1**), which can be conveniently isolated and characterized (Tables 1 and 2). The addition of two equivalents of the complex $[MX(PPh_3)]$ (M = Cu or Au, X = Cl; M = Ag, X = I) to a thf solution of $K_2[Ru_3(\mu_3\text{-}S)(CO)_9]$, in the presence of $TlPF_6$, affords a mixture of cluster compounds,

† 1,2-μ-[Bis(diphenylphosphino)methane] 3,3,3,4,4,4,5,5,5-nonacarbonyl-3,4,5-μ_3-sulphido-cyclo-dicoppertriruthenium(*Cu–Cu*)(5*Cu–Ru*)(3*Ru–Ru*) and -digoldtriruthenium(*Au–Au*)(4*Au–Ru*)(3*Ru–Ru*), respectively.

Supplementary data available: see Instructions for Authors, *J. Chem. Soc., Dalton Trans.*, 1987, Issue 1, pp. xvii—xx.

$[MRu_3(\mu\text{-}H)(\mu_3\text{-}S)(CO)_9(PPh_3)]$ [for M = Cu (**2**), Ag (**3**), or Au (**4**)], $[MRu_3(\mu\text{-}H)(\mu_3\text{-}S)(CO)_8(PPh_3)_2]$ [for M = Cu (**5**) or Ag (**6**)], and $[M_2Ru_3(\mu_3\text{-}S)(CO)_9(PPh_3)_2]$ [for M = Cu (**8**), Ag (**9**), or Au (**10**)]. The components of each mixture can be readily separated by column chromatography on Florisil or alumina, as appropriate. Unfortunately, in the case of copper and silver, the desired pentanuclear species (**8**) (11%) and (**9**) (7%) can only be obtained in very poor yield and the major product from the reaction is the phosphine-substituted tetranuclear cluster (**5**) (53%) or (**6**) (43%). Both reactions afford another tetranuclear cluster, without a PPh_3 group attached to ruthenium, although the silver species (**3**) (25%) is produced in much higher yield than the copper cluster (**2**) (8%). A much better yield (58%) of the pentanuclear species (**10**) is obtained, together with a small amount (7%) of the tetranuclear cluster (**4**), when $K_2[Ru_3(\mu_3\text{-}S)(CO)_9]$ is treated with $[AuCl(PPh_3)]$. Interestingly, the known[3] phosphine-substituted tetranuclear cluster $[AuRu_3(\mu\text{-}H)(\mu_3\text{-}S)(CO)_8(PPh_3)_2]$ (**7**) is not produced in the reaction.

All of the new clusters were characterized by microanalysis and spectroscopic measurements (Tables 1 and 2) and the ^1H and $^{31}P\text{-}\{^1H\}$ n.m.r. spectra obtained for the known species (**4**) and (**10**) are identical with those previously reported.[3] The very close similarity between the i.r. and n.m.r. spectroscopic data for the tetranuclear clusters (**2**)—(**4**) implies that the copper and silver congeners (**2**) and (**3**) adopt the same 'butterfly' metal-

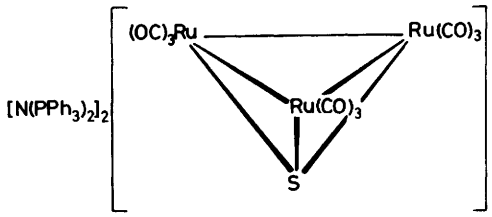

(**1**)

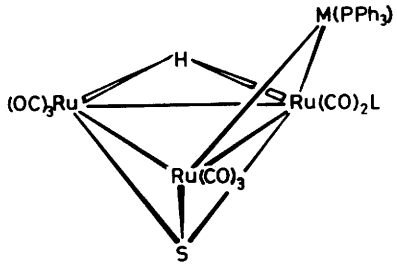

(**2**) M = Cu, L = CO
(**3**) M = Ag, L = CO
(**4**) M = Au, L = CO
(**5**) M = Cu, L = PPh_3
(**6**) M = Ag, L = PPh_3
(**7**) M = Au, L = PPh_3

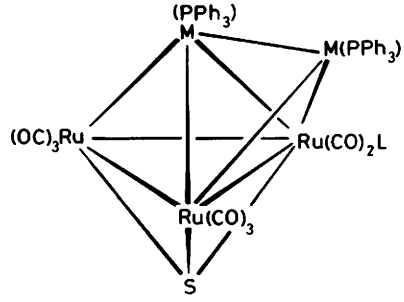

(**8**) M = Cu, L = CO
(**9**) M = Ag, L = CO
(**10**) M = Au, L = CO
(**11**) M = Au, L = PPh_3

Table 1. Analytical[a] and physical data for the new cluster compounds

Compound	M.p. (θ_c/°C) (decomp.)	$\nu_{max.}$(CO)[b]/cm^{-1}	Yield[c] (%)	Analysis (%) C	H
(**1**) $[N(PPh_3)_2]_2[Ru_3(\mu_3\text{-}S)(CO)_9]$	173—178	2 061w, 2 031vs, 1 997vs, 1 972s br, 1 918w br	82	[d]58.1 (58.4)	3.9 (3.6)
(**2**) $[CuRu_3(\mu\text{-}H)(\mu_3\text{-}S)(CO)_9(PPh_3)]$	127—131	[e]2 083m, 2 062vs, 2 035vs, 2 004s, 1 986vs, 1 933m	8	35.6 (35.5)	2.0 (1.8)
(**3**) $[AgRu_3(\mu\text{-}H)(\mu_3\text{-}S)(CO)_9(PPh_3)]$	138—142	[e]2 086m, 2 063vs, 2 038vs, 2 000s, 1 990s, 1 979s, 1 943m	25	33.9 (33.8)	1.6 (1.7)
(**5**) $[CuRu_3(\mu\text{-}H)(\mu_3\text{-}S)(CO)_8(PPh_3)_2]$	156—160	2 065m, 2 030vs, 2 007s, 1 968m br, 1 938m br, 1 921 (sh)	53	45.9 (46.0)	3.0 (2.7)
(**6**) $[AgRu_3(\mu\text{-}H)(\mu_3\text{-}S)(CO)_8(PPh_3)_2]$	162—166	[e]2 064m, 2 032vs, 2 011s, 1 986m, 1 975 (sh), 1 965s, 1 936s, 1 928 (sh)	43	44.1 (44.3)	2.9 (2.6)
(**7**) $[AuRu_3(\mu\text{-}H)(\mu_3\text{-}S)(CO)_8(PPh_3)_2]$[f,g]	178—182	[e]2 065m, 2 033vs, 2 015s, 1 988m, 1 977vs, 1 950m br		41.4 (41.2)	2.6 (2.4)
(**8**) $[Cu_2Ru_3(\mu_3\text{-}S)(CO)_9(PPh_3)_2]$	189—193	2 057m, 2 023vs, 2 013 (sh), 1 967m, 1 940s br	11	43.5 (43.6)	2.5 (2.4)
(**9**) $[Ag_2Ru_3(\mu_3\text{-}S)(CO)_9(PPh_3)_2]$	194—198	2 057m, 2 022vs, 2 014(sh), 1 968m, 1 943s br	7	40.7 (40.7)	2.4 (2.3)
(**12**) $[Cu_2Ru_3(\mu_3\text{-}S)(\mu\text{-}Ph_2PCH_2PPh_2)(CO)_9]$	165—169	2 059m, 2 031vs, 2 017vs, 1 980m, 1 939s, 1 923 (sh)	46	37.0 (37.2)	2.0 (2.0)
(**13**) $[Au_2Ru_3(\mu_3\text{-}S)(\mu\text{-}Ph_2PCH_2PPh_2)(CO)_9]$	185—189	2 066m, 2 041vs, 2 025vs, 1 978m, 1 954s vbr	75	29.7 (29.9)	1.6 (1.6)

[a] Calculated values given in parentheses. [b] Measured in dichloromethane solution, unless otherwise stated. [c] Based on ruthenium reactant. [d] N, 1.7 (1.7%). [e] Measured in cyclohexane solution. [f] Cluster cannot be prepared from the salt $K_2[Ru_3(\mu_3\text{-}S)(CO)_9]$. [g] Cluster has not previously been obtained pure.[3]

Table 2. Hydrogen-1, phosphorus-31, and carbon-13 n.m.r. data[a] for the new cluster compounds

Complex	^1H[b]	^{31}P-{^1H}[c]	^{13}C-{^1H} (ambient temperature)[d]	^{13}C-{^1H} (low temperature)[d,e]
(1)	7.44—7.63 (m, Ph)		[f]198.2 (CO), 134.2 [C^4(Ph)], 132.6 [AA'X pattern, C^3(Ph), *N*(PC) 11], 129.9 [AA'X pattern, C^2(Ph), *N*(PC) 13], 127.5 [apparent d (AA'X pattern), C^1(Ph), *N*(PC) 108]	204.4 (br, 3 CO), 195.0 (br, 6 CO)
(2)	[g] −18.52 (s br, 1 H, μ-H), 7.36—7.53 (m, 15 H, Ph)	4.9(s)	193.7 (CO), 134.2 [d, C^2(Ph), *J*(PC) 14], 131.4 [C^4(Ph)], 130.4 [d, C^1(Ph), *J*(PC) 40], 129.5 [d, C^3(Ph) *J*(PC) 10]	*ca.* 194 (vbr)
(3)	[h] −19.65 (s, 1 H, μ-H), 7.35—7.54 (m, 15 H, Ph)	[i]14.5 [2 x d, *J*(^{109}AgP) 481, *J*(^{107}AgP) 417]	[j]193.8 (CO), 133.9 [d, C^2(Ph), *J*(PC) 16], 131.3 [C^4(Ph)], 130.2 [d, C^1(Ph), *J*(PC) 35], 129.5 [d, C^3(Ph), *J*(PC) 10]	*ca.* 193 (vbr)
(5)	−17.79 [overlapping d of d, 1 H, μ-H, *J*(PH) 6], 7.36—7.50 (m, 30 H, Ph)	32.2 [d, PPh_3Ru, *J*(PP) 13], 4.1 [d, PPh_3Cu, *J*(PP) 13]	199.7 (vbr, CO), 195.9 (br, CO), 135.1 [d, C^1(RuPPh), *J*(PC) 43], 134.3 [d, C^2(CuPPh), *J*(PC) 14], 133.9 [d, C^2(RuPPh), *J*(PC) 11], 131.2 [d, C^1(CuPPh), *J*(PC) 38], 131.0 [C^4(CuPPh)], 130.7 [C^4(RuPPh)], 129.3 [d, C^3(CuPPh), *J*(PC) 10], 128.7 [d, C^3(RuPPh), *J*(PC) 10]	203.1 (1 CO), 199.1 (1 CO), 198.5 (br, 3 CO), 196.9 (1 CO), 194.0 (1 CO), 186.1 (1 CO)
(6)	[k] −18.56 [d, 1 H, μ-H, *J*(PH) 7], 7.24—7.67 (m, 30 H, Ph)	32.3 [2 x d of d, PPh_3Ru, *J*(^{109}AgP) 35, *J*(^{107}AgP) 32, *J*(PP) 23], 13.0 [2 x d of d, PPh_3Ag, *J*(^{109}AgP) 472, *J*(^{107}AgP) 408, *J*(PP) 23]	[l]196.3 (br, CO), 134.9 [d, C^1(RuPPh), *J*(PC) 44], 133.9 [d, C^2(AgPPh), *J*(PC) 16], 133.8 [d, C^2(RuPPh), *J*(PC) 12], 131.0 [C^4(AgPPh)], 130.9 [d, C^1(AgPPh), *J*(PC) 33], 130.4 [C^4(RuPPh)], 129.3 [d, C^3(AgPPh), *J*(PC) 10], 128.4 [d, C^3(RuPPh), *J*(PC) 10]	[m]204.5 (1 CO), 199.4 (1 CO), 197.9 (br, 3 CO), 193.8 (1 CO), 193.4 (1 CO), 187.4 (1 CO)
(8)	7.12—7.46 (m, Ph)	[n]0.8(s)		
(9)	7.05—7.52 (m, Ph)	[i]13.5 [m, ^1J(^{109}AgP) 440, ^1J(^{107}AgP) 382, ^2J(^{109}AgP)5, ^2J(^{107}AgP)4, J(^{109}Ag-^{109}Ag) 31, J(^{109}Ag-^{107}Ag) 27, J(^{107}Ag^{107}Ag) 24, *J*(PP) 0]		
(12)	3.35 [t, 2 H, PCH_2P, *J*(PH) 11], 7.42 (m, 20 H, Ph)	−7.5 (s)	[f]196.6 [t, CO, *J*(PC) 4], 133.0 [apparent t (AA'X pattern), C^2(Ph), *N*(PC) 15], 131.4 [C^4(Ph)], 131.2 [apparent t (AA'X pattern), C^1(Ph), *N*(PC) 41], 129.3 [apparent t (AA'X pattern), C^3(Ph), *N*(PC) 11], 26.3 [t, PCH_2P, *J*(PC) 15]	[m]*ca.* 195—192 (m, vbr)
(13)	3.58 [t, 2 H, PCH_2P, *J*(PH) 11], 7.36 (m, 20 H, Ph)	50.8(s)	[f]199.5 [t, CO, *J*(PC) 4], 133.1 [br, C^2(Ph)], 131.5 [C^4(Ph)], 131.5 [apparent t (AA'X pattern), C^1(Ph), *N*(PC) 41], 129.1 [br, C^3(Ph)], 29.2 [t, PCH_2P, *J*(PC) 20]	[m]198.6 (br)

[a] Chemical shifts (δ) in p.p.m., coupling constants in Hz. [b] Measured in [$^2H_2$]dichloromethane solution at ambient temperature, unless otherwise stated. [c] Hydrogen-1 decoupled, measured in [$^2H_2$]dichloromethane solution at −90 °C, unless otherwise stated; chemical shifts positive to high frequency of 85% H_3PO_4 (external). [d] Hydrogen-1 decoupled, measured in [$^2H_2$]dichloromethane–CH_2Cl_2 solution; chemical shifts positive to high frequency of $SiMe_4$. [e] Measured at −90 °C, unless otherwise stated. [f] *N*(PC) = |*J*(PC) + *J*(P'C)|. [g] μ-H at −40 °C, δ −18.21 [d, 1 H, *J*(PH) 8 Hz]. [h] Measured at −90 °C. [i] Measured at −50 °C. [j] ^{13}C-{^1H} N.m.r. data at ambient temperature for previously reported[3] analogous gold cluster, (4): δ 194.7 [d, CO, *J*(PC) 4], 134.0 [d, C^2(Ph), *J*(PC) 15], 131.5 [C^4(Ph)], 131.3 [d, C^1(Ph), *J*(PC) 47], 129.3 [d, C^3(Ph), *J*(PC) 11]; CO signals at −100 °C, *ca.* δ 193 (vbr). [k] μ-H at −90 °C, δ −18.96 [d, br, 1 H, *J*(PH) 4]. [l] ^{13}C-{^1H} N.m.r. data at ambient temperature for the previously reported[3] (but not obtained pure) analogous gold cluster, (7): δ 197.1 (vbr, CO), 134.8 [d, C^1(RuPPh), *J*(PC) 44], 134.2 [d, C^2(AuPPh), *J*(PC) 15], 134.0 [d, C^2(RuPPh), *J*(PC) 11], 132.1 [d, C^1(AuPPh), *J*(PC) 47], 131.2 [C^4(AuPPh)], 130.6 [C^4(RuPPh)], 129.2 [d, C^3(AuPPh), *J*(PC) 11], 128.5 [d, C^3(RuPPh), *J*(PC) 10]; CO signals at −90 °C, δ 207.6 (1 CO), 199.3 (br, 4 CO), 192.9 (1 CO), 191.5 (1 CO), and 187.8 (1 CO). [m] Measured at −100 °C. [n] At −90 °C, δ 0.6 (vbr).

core geometry as that previously established[3,4] for the corresponding gold compound (4). Likewise, the i.r. and n.m.r. spectroscopic data for the phosphine-substituted tetranuclear clusters (5) and (6) closely resemble those for the previously reported[3] gold analogue (7), suggesting a common metal-core geometry for all three clusters. The structure of (7) is thought[3] to be very similar to that of (4), but with a CO ligand in one of the $Ru(CO)_3$ groups replaced by a PPh_3 ligand. The phosphorus atom of the $M(PPh_3)$ moiety in (5)—(7) shows coupling to the hydrido ligand and to the other PPh_3 group, implying that the $Ru(CO)_2(PPh_3)$ fragment is attached to both the hydrido ligand and the $M(PPh_3)$ unit in each cluster. In order to confirm the formulations of compounds (5)—(7), they were independently prepared (*ca.* 80%) by treating the appropriate cluster (2)—(4) with PPh_3.

The close similarity of the i.r. spectra for the pentanuclear clusters (8)—(10) suggests that the copper and silver species (8) and (9) adopt the same trigonal-bipyramidal metal framework as that previously established[4] for the gold cluster (10), with one coinage metal occupying an equatorial site and the other an axial site. The ^{31}P-{^1H} n.m.r. spectrum of (9) at −50 °C is a complex multiplet, but analysis demonstrates that it consists of a single averaged phosphorus resonance split by $^{107,109}Ag$–^{31}P couplings through one and two bonds and also by $^{107,109}Ag$–$^{107,109}Ag$ couplings. If the two silver atoms are undergoing site-exchange, three different molecules of (9) are possible from

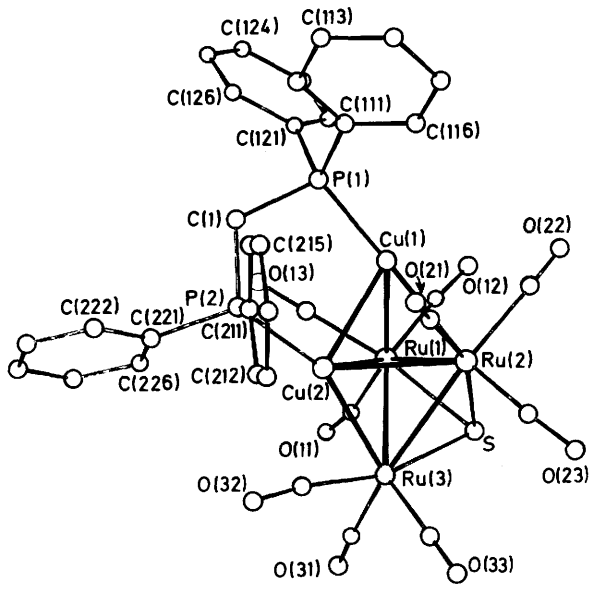

Figure 1. Molecular structure of $[Cu_2Ru_3(\mu_3\text{-}S)(\mu\text{-}Ph_2PCH_2PPh_2)(CO)_9]$ (**12**), showing the crystallographic numbering. The carbon atom of each carbonyl group has the same number as the oxygen atom

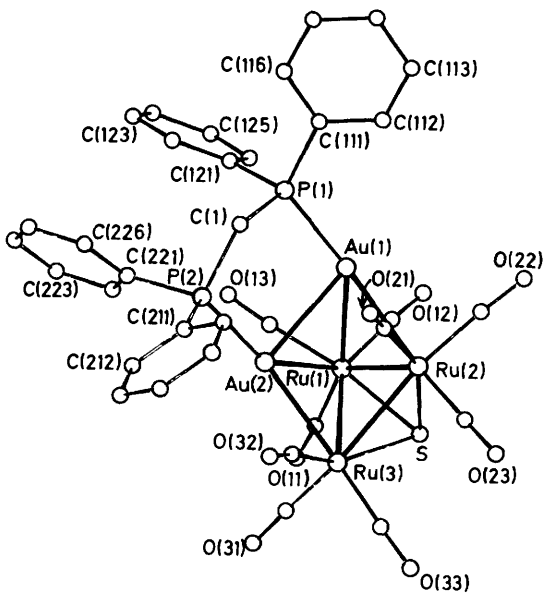

Figure 2. Molecular structure of $[Au_2Ru_3(\mu_3\text{-}S)(\mu\text{-}Ph_2PCH_2PPh_2)(CO)_9]$ (**13**), showing the crystallographic numbering. The carbon atom of each carbonyl group has the same number as the oxygen atom

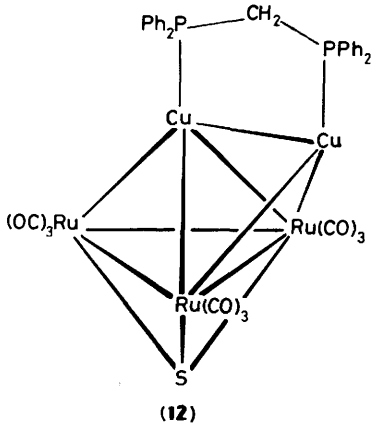

(**12**)

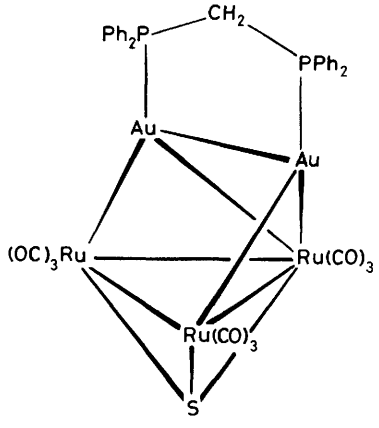

(**13**)

the various combinations of silver isotopes. The subspectrum of each of these isotopomers can be simulated using the A part of an AA'XX' or AA'MX spin system, as appropriate.[5] When the sub-spectra are all summed together, with the appropriate statistical weighting for the relative isotopic abundances, a very good fit with the observed spectrum of (**9**) is obtained. The magnitudes of $J(^{107,109}Ag\text{–}^{107,109}Ag)$ (24–31 Hz) for the pentanuclear Ag_2Ru_3 cluster (**9**) are of the same order as those reported (30–45 Hz)[5] for the hexanuclear species $[Ag_2Ru_4(\mu_3\text{-}H)_2\{\mu\text{-}Ph_2P(CH_2)_nPPh_2\}(CO)_{12}]$ (n = 1, 2, or 4). As the metal skeletons of the Ag_2Ru_4 clusters all contain a trigonal-bipyramidal Ag_2Ru_3 unit, with adjacent silver atoms in close contact,[5,6] these data support the structure proposed for the Ag_2Ru_3 core in (**9**). At ambient temperature, an averaged phosphorus environment is also observed in the $^{31}P\text{-}\{^1H\}$ n.m.r. spectrum of the analogous Cu_2Ru_3 compound (**8**), so both (**8**) and (**9**) are undergoing a similar intramolecular metal-core rearrangement to that previously observed[3] for the gold cluster (**10**). Unlike the spectrum of (**9**), which is not significantly broadened even at −90 °C, the singlet exhibited by (**8**) is very severely broadened at this temperature, suggesting a higher free energy of activation ($\Delta G^{\ddagger}$) for the fluxion in the copper species. Similar trends in $\Delta G^{\ddagger}$ have been observed previously[6,7] for other series of Group 1B metal congeners.

At ambient temperature, $^{13}C\text{-}\{^1H\}$ n.m.r. studies (Table 2) show that all of the clusters (**1**)—(**9**) are undergoing dynamic behaviour involving CO site-exchange. At −90 °C, a spectrum consistent with the ground-state structure can be obtained for the salt (**1**), but for all the other clusters it is not possible to stop the fluxional process completely, even at −90 or −100 °C. In addition, variable-temperature ^1H and $^{31}P\text{-}\{^1H\}$ n.m.r. spectroscopic studies (Table 2) demonstrate that the PPh_3 group(s) in the copper–ruthenium species (**2**) and the silver–ruthenium clusters (**3**), (**6**), and (**9**) are undergoing intermolecular exchange between clusters at ambient temperature. This type of dynamic behaviour has been observed previously for a number of heteronuclear silver clusters[2,7] and also for one mixed-metal copper cluster.[2]

Treatment of a thf solution of $K_2[Ru_3(\mu_3\text{-}S)(CO)_9]$ with a dichloromethane solution of the complex $[M_2(\mu\text{-}Ph_2PCH_2PPh_2)Cl_2]$ (M = Cu or Au), in the presence of $TlPF_6$, affords good yields of the pentanuclear clusters $[M_2Ru_3(\mu_3\text{-}S)(\mu\text{-}Ph_2PCH_2PPh_2)(CO)_9]$ [M = Cu (**12**) or Au (**13**)], as dark

Table 3. Selected bond lengths (Å), with estimated standard deviations in parentheses, for $[M_2Ru_3(\mu_3\text{-}S)(\mu\text{-}Ph_2PCH_2PPh_2)(CO)_9]$ [M = Cu (**12**) or Au (**13**)]

	(12)	(13)		(12)	(13)
Ru(1)–Ru(2)	2.856(2)	2.968(2)	Ru(1)–Ru(3)	2.837(3)	2.923(1)
Ru(1)–M(1)	2.654(2)	2.792(1)	Ru(1)–M(2)	2.745(3)	2.836(1)
Ru(1)–S	2.357(5)	2.340(3)	Ru(1)–C(11)	1.944(21)	1.838(20)
Ru(1)–C(12)	2.081(22)	1.871(15)	Ru(1)–C(13)	1.904(17)	1.915(15)
Ru(2)–Ru(3)	2.814(2)	2.773(2)	Ru(2)–M(1)	2.597(3)	2.785(1)
Ru(2)–M(2)	2.794(2)	3.335(1)	Ru(2)–S	2.348(5)	2.339(4)
Ru(2)–C(21)	1.819(19)	1.918(13)	Ru(2)–C(22)	1.857(21)	1.885(16)
Ru(2)–C(23)	1.845(22)	1.846(14)	Ru(3)–M(2)	2.552(2)	2.742(1)
Ru(3)–S	2.336(6)	2.359(4)	Ru(3)–C(31)	1.910(20)	1.872(19)
Ru(3)–C(32)	1.870(23)	1.881(17)	Ru(3)–C(33)	1.919(25)	1.842(15)
M(1)–M(2)	2.515(3)	2.802(1)	M(1)–P(1)	2.214(5)	2.307(3)
M(2)···C(32)	2.274(23)	2.543(15)	M(2)–P(2)	2.231(5)	2.315(3)
C(11)–O(11)	1.082(25)	1.18(3)	C(12)–O(12)	1.00(3)	1.158(20)
C(13)–O(13)	1.153(21)	1.129(20)	C(21)–O(21)	1.215(23)	1.129(17)
C(22)–O(22)	1.17(3)	1.172(23)	C(23)–O(23)	1.15(3)	1.169(19)
C(31)–O(31)	1.146(25)	1.145(23)	C(32)–O(32)	1.18(3)	1.162(22)
C(33)–O(33)	1.13(3)	1.176(19)	P(1)–C(1)	1.850(16)	1.850(12)
P(1)–C(111)	1.775(10)	1.818(10)	P(1)–C(121)	1.863(14)	1.815(11)
P(2)–C(1)	1.840(17)	1.852(14)	P(2)–C(211)	1.777(12)	1.826(8)
P(2)–C(221)	1.828(9)	1.820(11)			

orange *microcrystals* (46%) for (**12**) and red *microcrystals* (75%) for (**13**). The analytical and spectroscopic data (Tables 1 and 2) for the two clusters are fully consistent with the proposed formulations.

X-Ray diffraction studies of the two pentanuclear clusters (**12**) and (**13**) show the molecular structures illustrated in Figures 1 and 2, respectively. Selected bond lengths for the two compounds are summarized in Table 3, and selected angles in Table 4. The Cu_2Ru_3 metal skeleton of (**12**) has a distorted trigonal-bipyramidal geometry, with Cu(1) occupying an axial site and Cu(2) being equatorial. This structure is similar to that established previously for the Au_2Ru_3 clusters (**10**) and (**11**).[3,4] In contrast, the metal core of the new Au_2Ru_3 cluster (**13**) may be regarded as derived from this type of geometry by the breaking of one equatorial metal–metal contact [Au(2) ··· Ru(2) 3.335(1) Å] to give an overall structure intermediate between a trigonal bipyramid and a square-based pyramid. The ligand distributions in (**12**) and (**13**) are similar, with each cluster having a bidentate $Ph_2PCH_2PPh_2$ ligand spanning the M(1)–M(2) bond, the S atom capping the Ru_3 face, and the CO ligands essentially linear.

The bridged Cu(1)–Cu(2) distance in (**12**) [2.515(3) Å] is significantly shorter than the unbridged distances reported in the heteronuclear clusters $[Cu_2Ru_4(\mu_3\text{-}H)_2(CO)_{12}(PPh_3)_2]$ [2.699(2) Å][7] and $[Cu_2Ru_6C(CO)_{16}(NCMe)_2]$ [mean reported value, 2.691(1) Å],[8] but is closer to the shorter Cu–Cu separations in the homonuclear species $[Cu_6H_6(PR_3)_6]$ (R = Ph or *p*-tolyl) [2.494—2.595(5) Å][9] and $[Cu_8H_8\{\mu\text{-}Ph_2P(CH_2)_3PPh_2\}_4]$ [2.453—2.517(3) Å].[10] The Au(1)–Au(2) distance in (**13**) [2.802(1) Å] is significantly shorter than that observed for the unbridged Au–Au contacts in (**10**) [2.967(2) Å][4] and (**11**) [2.915(2) Å],[3] but it is similar to the lengths of the bridged Au–Au vectors in $[Au_2Ru_4(\mu_3\text{-}H)(\mu\text{-}H)(\mu\text{-}Ph_2PCH_2PPh_2)(CO)_{12}]$ [2.823(1) Å][6] and $[Au_3Ru_4(\mu\text{-}H)(\mu\text{-}Ph_2PCH_2PPh_2)(CO)_{12}(PPh_3)]$ [2.758(2) Å].[11]

The equatorial Cu–Ru separations in (**12**) [Cu(2)–Ru(1) 2.745(3) and Cu(2)–Ru(2) 2.794(2) Å] are significantly longer than the corresponding axial distances [Cu(1)–Ru(1) 2.654(2), Cu(1)–Ru(2) 2.597(3), and Cu(2)–Ru(3) 2.552(2) Å]. Previously reported[7,8,12] unbridged Cu–Ru distances show a similar range of lengths [2.577—2.741(1) Å]. The 'equatorial' Au–Ru separations in the gold cluster (**13**) [Au(2)–Ru(1) 2.836(1) and Au(2)··· Ru(2) 3.335(1) Å] are also significantly longer than the 'axial' distances [Au(1)–Ru(1) 2.792(1), Au(1)–Ru(2) 2.785(1), and Au(2)–Ru(3) 2.742(1) Å]. In this case, the Au(2)··· Ru(2) 'equatorial' distance is too long to indicate significant bonding interaction, so that the metal skeleton of (**13**) is distorted from trigonal bipyramidal towards square-based pyramidal geometry. The four atoms that form the 'square base' in the pyramidal description of the geometry show marked tetrahedral distortion from exact planarity [deviations from the mean plane: Ru(2) and Au(2) 0.25, and Ru(3) and Au(1) −0.25 Å], and the metal framework is best envisaged as intermediate between a trigonal bipyramid and a square-based pyramid. There are two other examples of a change in the metal-core geometry of a heteronuclear cluster on replacement of two PPh_3 groups attached to gold atoms by a $Ph_2PCH_2PPh_2$ ligand. The monocapped trigonal-bipyramidal metal skeleton of the hexanuclear species $[Au_2Ru_4(\mu_3\text{-}H)(\mu\text{-}H)(CO)_{12}(PPh_3)_2]$ and the bicapped trigonal-bipyramidal metal framework of the heptanuclear cluster $[Au_3Ru_4(\mu_3\text{-}H)(CO)_{12}(PPh_3)_3]$ are altered to somewhat distorted mono- or bi-capped square-based pyramidal geometries, respectively, by this type of ligand change.[6,11]

The Cu–P and Au–P bond lengths [mean 2.221(5) and 2.311(3) Å, respectively] are similar to those observed in related compounds.[2–4,7,11,13,14] The Ru–S bond lengths in (**12**) and (**13**) do not differ significantly from their mean values (2.346 Å), which are the same in both clusters.

The metal–carbonyl angles in both compounds are in the normal range observed for terminal CO ligands [M–C–O 167—179° for (**12**) and 168–179° for (**13**)]. In both (**12**) and (**13**), there is an extremely short contact between CO(32), attached to the apical Ru(3) atom, and the coinage metal M(2) [Cu(2)··· C(32) 2.274(23) and Au(2)··· C(32) 2.543(15) Å]. Very short M–C contacts between Cu atoms[2,8,15] or Au atoms[3,14–16] and essentially linear CO ligands bonded to adjacent metals have been reported before in heteronuclear clusters.

A single resonance is observed in the ambient-temperature $^{31}P\text{-}\{^1H\}$ n.m.r. spectra of (**12**) and (**13**) and, in each case, the signal is still a sharp singlet at −90 °C. Thus, the intramolecular core rearrangement which exchanges the coinage metals between the two distinct sites in the metal skeletons of (**8**)—(**11**) still occurs when the two Group 1B metals are linked together by a bidentate phosphine ligand in (**12**) and (**13**). In addition, it is of special interest that the metal-core geometry adopted by

Table 4. Selected bond angles (°), with estimated standard deviations in parentheses, for $[M_2Ru_3(\mu_3\text{-}S)(\mu\text{-}Ph_2PCH_2PPh_2)(CO)_9]$ [M = Cu (**12**) or Au (**13**)]

	(12)	(13)		(12)	(13)
Ru(3)–Ru(1)–Ru(2)	59.2(1)	56.1(1)	M(1)–Ru(1)–Ru(2)	56.1(1)	57.7(1)
M(1)–Ru(1)–Ru(3)	100.3(1)	98.2(1)	M(2)–Ru(1)–Ru(2)	59.8(1)	70.1(1)
M(2)–Ru(1)–Ru(3)	54.4(1)	56.8(1)	M(2)–Ru(1)–M(1)	55.5(1)	59.7(1)
S–Ru(1)–Ru(2)	52.5(1)	50.6(1)	S–Ru(1)–Ru(3)	52.5(1)	51.8(1)
S–Ru(1)–M(1)	107.3(1)	107.1(1)	S–Ru(1)–M(2)	96.7(2)	103.6(1)
C(11)–Ru(1)–Ru(2)	148.9(7)	137.6(5)	C(11)–Ru(1)–Ru(3)	95.1(7)	89.8(5)
C(11)–Ru(1)–M(1)	153.8(6)	163.2(6)	C(11)–Ru(1)–M(2)	121.6(7)	114.5(6)
C(11)–Ru(1)–S	98.9(6)	89.5(5)	C(12)–Ru(1)–Ru(2)	100.1(5)	97.7(6)
C(12)–Ru(1)–Ru(3)	147.9(5)	145.7(5)	C(12)–Ru(1)–M(1)	84.2(5)	81.9(4)
C(12)–Ru(1)–M(2)	139.7(5)	140.7(4)	C(12)–Ru(1)–S	95.7(5)	95.0(5)
C(12)–Ru(1)–C(11)	93.9(9)	99.8(7)	C(13)–Ru(1)–Ru(2)	117.8(5)	126.7(5)
C(13)–Ru(1)–Ru(3)	113.8(6)	118.9(4)	C(13)–Ru(1)–M(1)	67.2(5)	73.1(5)
C(13)–Ru(1)–M(2)	68.7(6)	68.2(4)	C(13)–Ru(1)–S	165.2(6)	170.7(4)
C(13)–Ru(1)–C(11)	87.3(8)	90.1(7)	C(13)–Ru(1)–C(12)	97.3(8)	94.2(6)
Ru(3)–Ru(2)–Ru(1)	60.1(1)	61.1(1)	M(1)–Ru(2)–Ru(1)	58.0(1)	57.9(1)
M(1)–Ru(2)–Ru(3)	102.3(1)	102.1(1)	M(2)–Ru(2)–Ru(1)	58.1(1)	53.1(1)
M(2)–Ru(2)–Ru(3)	54.1(1)	52.4(1)	M(2)–Ru(2)–M(1)	55.5(1)	53.6(1)
S–Ru(2)–Ru(1)	52.8(1)	50.7(1)	S–Ru(2)–Ru(3)	52.9(1)	54.2(1)
S–Ru(2)–M(1)	109.5(1)	107.3(1)	S–Ru(2)–M(2)	95.6(1)	90.2(1)
C(21)–Ru(2)–Ru(1)	118.0(6)	117.9(5)	C(21)–Ru(2)–Ru(3)	107.7(6)	101.9(5)
C(21)–Ru(2)–M(1)	68.7(6)	71.1(4)	C(21)–Ru(2)–M(2)	66.8(5)	69.2(5)
C(21)–Ru(2)–S	160.3(6)	155.8(5)	C(22)–Ru(2)–Ru(1)	95.2(6)	102.5(5)
C(22)–Ru(2)–Ru(3)	149.7(6)	157.1(5)	C(22)–Ru(2)–M(1)	74.5(6)	79.1(4)
C(22)–Ru(2)–M(2)	129.9(6)	132.6(4)	C(22)–Ru(2)–S	98.9(6)	103.4(4)
C(22)–Ru(2)–C(21)	99.3(8)	100.0(6)	C(23)–Ru(2)–Ru(1)	143.4(6)	139.2(5)
C(23)–Ru(2)–Ru(3)	95.0(6)	87.3(5)	C(23)–Ru(2)–M(1)	158.4(6)	162.0(4)
C(23)–Ru(2)–M(2)	130.7(7)	127.1(5)	C(23)–Ru(2)–S	91.2(6)	90.6(5)
C(23)–Ru(2)–C(21)	94.0(9)	92.0(6)	C(23)–Ru(2)–C(22)	96.7(9)	98.3(7)
Ru(2)–Ru(3)–Ru(1)	60.7(1)	62.7(1)	M(2)–Ru(3)–Ru(1)	61.0(1)	60.0(1)
M(2)–Ru(3)–Ru(2)	62.5(1)	74.4(1)	S–Ru(3)–Ru(1)	53.1(1)	51.3(1)
S–Ru(3)–Ru(2)	53.3(1)	53.5(1)	S–Ru(3)–M(2)	102.8(1)	106.0(1)
C(31)–Ru(3)–Ru(1)	96.4(8)	93.2(4)	C(31)–Ru(3)–Ru(2)	149.7(8)	155.3(4)
C(31)–Ru(3)–M(2)	126.2(6)	99.2(4)	C(31)–Ru(3)–S	97.7(7)	108.0(4)
C(32)–Ru(3)–Ru(1)	112.1(7)	123.4(4)	C(32)–Ru(3)–Ru(2)	112.8(6)	98.8(6)
C(32)–Ru(3)–M(2)	59.5(7)	63.6(4)	C(32)–Ru(3)–S	162.3(7)	152.1(7)
C(32)–Ru(3)–C(31)	93.6(9)	99.5(8)	C(33)–Ru(3)–Ru(1)	150.3(7)	143.1(5)
C(33)–Ru(3)–Ru(2)	94.1(6)	102.6(6)	C(33)–Ru(3)–M(2)	123.8(7)	153.1(5)
C(33)–Ru(3)–S	100.0(7)	92.2(5)	C(33)–Ru(3)–C(31)	100.2(9)	93.6(7)
C(33)–Ru(3)–C(32)	91(1)	91.1(7)	Ru(2)–M(1)–Ru(1)	65.9(1)	64.3(1)
M(2)–M(1)–Ru(1)	64.1(1)	60.9(1)	M(2)–M(1)–Ru(2)	66.2(1)	73.3(1)
P(1)–M(1)–Ru(1)	138.0(1)	140.2(1)	P(1)–M(1)–Ru(2)	148.4(2)	143.7(1)
P(1)–M(1)–M(2)	102.6(1)	95.7(1)	Ru(2)–M(2)–Ru(1)	62.1(1)	56.8(1)
Ru(3)–M(2)–Ru(1)	64.7(1)	63.2(1)	Ru(3)–M(2)–Ru(2)	63.3(1)	53.2(1)
M(1)–M(2)–Ru(1)	60.4(1)	59.4(1)	M(1)–M(2)–Ru(2)	58.3(1)	53.1(1)
M(1)–M(2)–Ru(3)	112.6(1)	102.4(1)	C(32)–M(2)–Ru(1)	103.1(6)	104.5(4)
C(32)–M(2)–Ru(2)	101.4(5)	73.6(5)	C(32)–M(2)–Ru(3)	45.1(6)	41.5(4)
C(32)–M(2)–M(1)	157.6(6)	125.0(5)	P(2)–M(2)–Ru(1)	136.4(2)	143.3(1)
P(2)–M(2)–Ru(2)	134.6(1)	125.9(1)	P(2)–M(2)–Ru(3)	154.3(2)	152.3(1)
P(2)–M(2)–M(1)	92.9(1)	92.1(1)	P(2)–M(2)–C(32)	109.2(6)	111.1(4)
Ru(2)–S–Ru(1)	74.7(1)	78.7(1)	Ru(3)–S–Ru(1)	74.4(1)	76.9(1)
Ru(3)–S–Ru(2)	73.8(2)	72.3(1)	O(11)–C(11)–Ru(1)	171(2)	176(1)
O(12)–C(12)–Ru(1)	176(2)	176(1)	O(13)–C(13)–Ru(1)	173(2)	168(1)
O(21)–C(21)–Ru(2)	167(1)	169(1)	O(22)–C(22)–Ru(2)	177(2)	171(1)
O(23)–C(23)–Ru(2)	178(2)	177(1)	O(31)–C(31)–Ru(3)	179(2)	179(1)
M(2)–C(32)–Ru(3)	75.3(8)	74.9(5)	O(32)–C(32)–Ru(3)	167(2)	169(2)
O(32)–C(32)–M(2)	118(2)	114(1)	O(33)–C(33)–Ru(3)	177(2)	178(2)
C(1)–P(1)–M(1)	107.9(5)	106.3(3)	C(111)–P(1)–M(1)	117.3(4)	119.9(3)
C(111)–P(1)–C(1)	106.4(6)	105.2(5)	C(121)–P(1)–M(1)	115.2(4)	115.0(3)
C(121)–P(1)–C(1)	102.5(6)	106.3(6)	C(121)–P(1)–C(111)	106.2(5)	103.0(4)
C(1)–P(2)–M(2)	113.8(6)	112.2(4)	C(211)–P(2)–M(2)	113.7(4)	111.6(2)
C(211)–P(2)–C(1)	105.8(6)	104.1(5)	C(221)–P(2)–M(2)	116.6(3)	120.0(3)
C(221)–P(2)–C(1)	100.6(6)	103.9(5)	C(221)–P(2)–C(211)	105.0(5)	103.6(4)
P(2)–C(1)–P(1)	115.3(8)	116.0(7)			

(**13**) is actually somewhere in between the trigonal-bipyramidal structure of (**8**)—(**12**) and the square-based pyramidal structure of the intermediate required for a restricted Berry pseudo-rotation, the mechanism proposed[3] to explain the intra-molecular metal-core rearrangements in (**10**) and (**11**). The observation that the Au_2Ru_3 metal framework of (**13**) shows considerable distortion in the same manner as that required in this mechanism lends support to the proposed method of

coinage metal site-exchange. The restricted Berry pseudo-rotation mechanism is also consistent with the fact that the two gold atoms are still able to undergo pairwise exchange in the distorted metal framework of (**13**).

Experimental

The techniques used and the instrumentation employed have been described elsewhere.[2] Light petroleum refers to that fraction of b.p. 40—60 °C. Established methods were used to prepare $[Ru_3(\mu\text{-}H)_2(\mu_3\text{-}S)(CO)_9]$,[17] $[AgI(PPh_3)]$,[18] and $[M_2(\mu\text{-}Ph_2PCH_2PPh_2)Cl_2]$ (M = Cu[19] or Au[20]). The complexes $[MCl(PPh_3)]$ (M = Cu[21] or Au[22]) were synthesized by adaptation of published routes. Analytical and other physical data for the new compounds are presented in Table 1, together with their i.r. spectra, and Table 2 summarizes the results of n.m.r. spectroscopic measurements. Product separation by column chromatography was performed on Aldrich Florisil (100—200 mesh) or B.D.H. alumina (Brockman activity II).

Synthesis of $[N(PPh_3)_2]_2[Ru_3(\mu_3\text{-}S)(CO)_9]$.—An ethanol (15 cm^3) suspension of $[Ru_3(\mu\text{-}H)_2(\mu_3\text{-}S)(CO)_9]$ (0.25 g, 0.42 mmol) was treated with KOH (0.10 g, 1.80 mmol) and the mixture was stirred at 60 °C for 30 min. After filtration of the resultant dark red mixture through a Celite pad (*ca.* 1 × 3 cm), an ethanol (10 cm^3) solution of $[N(PPh_3)_2]Cl$ (0.50 g, 0.87 mmol) was added. The crude dark yellow product was collected by filtration onto a Celite pad (*ca.* 1 × 3 cm) and then washed successively with ethanol (3 × 10 cm^3) and diethyl ether (3 × 10 cm^3). To remove the KCl produced in the reaction, the crude product was extracted with dichloromethane (3 × 10 cm^3) and filtered through the Celite pad. Careful addition of light petroleum to this solution afforded yellow *microcrystals* of $[N(PPh_3)_2]_2[Ru_3(\mu_3\text{-}S)(CO)_9]$ (**1**) (0.58 g).

Reaction of $K_2[Ru_3(\mu_3\text{-}S)(CO)_9]$ *with* $[MX(PPh_3)]$ (M = Cu *or* Au, X = Cl; M = Ag, X = I).—A thf (80 cm^3) solution of $[Ru_3(\mu\text{-}H)_2(\mu_3\text{-}S)(CO)_9]$ (0.25 g, 0.42 mmol) was treated with an excess of KH (0.15 g, 3.8 mmol) and the mixture was allowed to stir overnight at ambient temperature. After filtration of the red-brown product through a Celite pad (*ca.* 1 × 3 cm), $[CuCl(PPh_3)]$ (0.31 g, 0.86 mmol) and $TlPF_6$ (0.60 g, 1.72 mmol) were added and the mixture was stirred for 1 h. A second filtration through a Celite pad (*ca.* 1 × 3 cm) was followed by the removal of the solvent under reduced pressure and the crude orange residue was dissolved in a dichloromethane–light petroleum mixture (1:4). Chromatography at −20 °C on a Florisil column (20 × 3 cm), eluting with a dichloromethane–light petroleum mixture (1:4), afforded three fractions, which after removal of the solvent under reduced pressure, yielded: (*i*) orange *microcrystals* of $[CuRu_3(\mu\text{-}H)(\mu_3\text{-}S)(CO)_9(PPh_3)]$ (**2**) (0.03 g), recrystallized from light petroleum; (*ii*) orange *microcrystals* of $[CuRu_3(\mu\text{-}H)(\mu_3\text{-}S)(CO)_8(PPh_3)_2]$ (**5**) (0.26 g), recrystallized from a dichloromethane–light petroleum mixture; (*iii*) dark orange *microcrystals* of $[Cu_2Ru_3(\mu_3\text{-}S)(CO)_9(PPh_3)_2]$ (**8**) (0.06 g), recrystallized from a dichloromethane–light petroleum mixture.

Orange *microcrystals* of $[AgRu_3(\mu\text{-}H)(\mu_3\text{-}S)(CO)_9(PPh_3)]$ (**3**) (0.10 g) and $[AgRu_3(\mu\text{-}H)(\mu_3\text{-}S)(CO)_8(PPh_3)_2]$ (**6**) (0.22 g) and dark orange *microcrystals* of $[Ag_2Ru_3(\mu_3\text{-}S)(CO)_9(PPh_3)_2]$ (**9**) (0.04 g) were similarly prepared, using $[AgI(PPh_3)]$ (0.42 g, 0.85 mmol) instead of $[CuCl(PPh_3)]$ and alumina instead of Florisil for the chromatography at −20 °C. When the same procedure was used with $[AuCl(PPh_3)]$ (0.42 g, 0.85 mmol) instead of $[CuCl(PPh_3)]$, and alumina at room temperature instead of Florisil at −20 °C for the chromatography, orange *crystals* of $[AuRu_3(\mu\text{-}H)(\mu_3\text{-}S)(CO)_9(PPh_3)]$ (**4**) (0.03 g) and red *crystals* of $[Au_2Ru_3(\mu_3\text{-}S)(CO)_9(PPh_3)_2]\cdot 0.5CH_2Cl_2$ (**10**) (0.38 g) were obtained.

Reaction of $[MRu_3(\mu\text{-}H)(\mu_3\text{-}S)(CO)_9(PPh_3)]$ (M = Cu, Ag, *or* Au) *with* PPh_3.—To a diethyl ether (30 cm^3) solution of $[CuRu_3(\mu\text{-}H)(\mu_3\text{-}S)(CO)_9(PPh_3)]$ (0.17 g, 0.19 mmol) was added powdered PPh_3 (0.05 g, 0.19 mmol) and the mixture was stirred for 2 h. After removal of the solvent under reduced pressure, the crude residue was dissolved in a dichloromethane–light petroleum mixture (1:4) and chromatographed on a Florisil column (15 × 2 cm) at −20 °C. Elution with a dichloromethane–light petroleum mixture (1:4) afforded a faint yellow fraction, followed by an intense orange fraction. After removal of the solvent from these fractions under reduced pressure, they were identified as unreacted starting material and $[CuRu_3(\mu\text{-}H)(\mu_3\text{-}S)(CO)_8(PPh_3)_2]$ (**5**) (0.17 g, 80%), respectively.

Similar treatment of $[AgRu_3(\mu\text{-}H)(\mu_3\text{-}S)(CO)_9(PPh_3)]$ (0.18 g, 0.19 mmol) or $[AuRu_3(\mu\text{-}H)(\mu_3\text{-}S)(CO)_9(PPh_3)]$ (0.20 g, 0.19 mmol), using the appropriate chromatography conditions as described in the previous section, afforded $[AgRu_3(\mu\text{-}H)(\mu_3\text{-}S)(CO)_8(PPh_3)_2]$ (**6**) (0.17 g, 76%) or $[AuRu_3(\mu\text{-}H)(\mu_3\text{-}S)(CO)_8(PPh_3)_2]$ (**7**) (0.19 g, 78%), respectively, together with small amounts of unreacted starting material.

Reaction of $K_2[Ru_3(\mu_3\text{-}S)(CO)_9]$ *with* $[M_2(\mu\text{-}Ph_2PCH_2PPh_2)Cl_2]$ (M = Cu *or* Au).—To a thf (50 cm^3) solution of $K_2[Ru_3(\mu_3\text{-}S)(CO)_9]$, prepared from $[Ru_3(\mu\text{-}H)_2(\mu_3\text{-}S)(CO)_9]$ (0.30 g, 0.51 mmol) as previously described, was added a dichloromethane (50 cm^3) solution of $[Cu_2(\mu\text{-}Ph_2PCH_2PPh_2)Cl_2]$ (0.30 g, 0.52 mmol) and solid $TlPF_6$ (0.70 g, 2.00 mmol). The mixture was stirred overnight and then filtered through a Celite pad (*ca.* 1 × 3 cm). After removal of the solvent under reduced pressure, the crude dark orange residue was dissolved in a dichloromethane–light petroleum mixture (1:2) and chromatographed on a Florisil column (20 × 3 cm) at −20 °C. Elution with a dichloromethane–light petroleum mixture (1:2) afforded a dark orange fraction containing the product. After removal of the solvent from this fraction under reduced pressure, crystallization of the residue from a dichloromethane–light petroleum mixture yielded dark orange *microcrystals* of $[Cu_2Ru_3(\mu_3\text{-}S)(\mu\text{-}Ph_2PCH_2PPh_2)(CO)_9]$ (**12**) (0.26 g).

Red *microcrystals* of $[Au_2Ru_3(\mu_3\text{-}S)(\mu\text{-}Ph_2PCH_2PPh_2)(CO)_9]$ (**13**) (0.52 g) were similarly prepared, using $[Au_2(\mu\text{-}Ph_2PCH_2PPh_2)Cl_2]$ (0.43 g, 0.51 mmol) instead of $[Cu_2(\mu\text{-}Ph_2PCH_2PPh_2)Cl_2]$, and alumina at room temperature instead of Florisil at −20 °C for the chromatography.

Crystal Structure Determination.—Crystals of $[M_2Ru_3(\mu_3\text{-}S)(\mu\text{-}Ph_2PCH_2PPh_2)(CO)_9]$ (M = Cu or Au) were grown from dichloromethane–light petroleum solutions by slow layer diffusion at −20 °C.

Crystal data for (**12**). $C_{34}H_{22}Cu_2O_9P_2Ru_3S$, M = 1 098.85, monoclinic, space group $C2/c$, a = 24.329(4), b = 10.926(2), c = 29.305(5) Å, β = 99.625(2)°, U = 7 680.16 Å^3, Z = 8, D_c = 1.900 g cm^{-3}, $F(000)$ = 4 272, λ(Mo-K_α) = 0.710 69 Å, μ(Mo-K_α) = 22.71 cm^{-1}.

Crystal data for (**13**). $C_{34}H_{22}Au_2O_9P_2Ru_3S$, M = 1 365.71, triclinic, space group $P\bar{1}$ (no. 2), a = 18.428(3), b = 11.067(2), c = 10.462(2) Å, α = 111.53(2), β = 79.47(2), γ = 108.09(2)°, U = 1 880.95 Å^3, Z = 2, D_c = 2.411 g cm^{-3}, $F(000)$ = 1 104, λ(Mo-K_α) = 0.710 69 Å, μ(Mo-K_α) = 87.36 cm^{-1}.

The data collection and processing methods for (**12**) and (**13**) were similar to those described previously.[23] The crystals selected for data collection had dimensions 0.22 × 0.20 × 0.18 and 0.28 × 0.15 × 0.13 mm for (**12**) and (**13**), respectively. A scan width of 0.70° was used to collect data in the θ range 25—33° for both crystals. For the gold compound (**13**), 360 azimuthal scan data were used in the absorption correction and the relative transmission factor varied from 1.00 to 0.47. The data for (**12**) were not corrected for absorption. Equivalent

Table 5. Fractional atomic co-ordinates for $[M_2Ru_3(\mu_3\text{-}S)(\mu\text{-}Ph_2PCH_2PPh_2)(CO)_9]$ [M = Cu (**12**) or Au (**13**)], with estimated standard deviations in parentheses

	(12)			(13)		
Atom	*x*	*y*	*z*	*x*	*y*	*z*
Ru(1)	0.088 31(6)	0.209 40(12)	0.054 15(6)	0.317 41(6)	−0.018 81(9)	−0.247 59(10)
Ru(2)	0.161 28(5)	0.168 91(12)	0.139 77(6)	0.307 00(6)	−0.209 02(9)	−0.101 47(10)
Ru(3)	0.046 05(6)	0.128 47(12)	0.133 53(7)	0.187 42(6)	−0.253 20(10)	−0.254 06(11)
M(1)	0.164 22(8)	0.369 45(17)	0.092 67(9)	0.341 26(3)	0.068 68(5)	0.031 63(5)
M(2)	0.078 90(8)	0.349 64(17)	0.130 19(8)	0.191 32(3)	−0.012 37(5)	−0.046 34(5)
S	0.107 0(2)	0.022 6(4)	0.093 9(2)	0.315 9(2)	−0.246 8(3)	−0.338 2(3)
P(1)	0.177 6(2)	0.569 9(4)	0.092 6(2)	0.320 7(2)	0.234 6(3)	0.235 3(3)
P(2)	0.077 9(2)	0.548 9(4)	0.146 5(2)	0.148 6(2)	0.117 0(3)	0.166 9(3)
C(11)	0.023 2(9)	0.159 7(19)	0.010 2(8)	0.296 3(10)	−0.028 0(16)	−0.416 4(17)
O(11)	−0.016 6(6)	0.140 7(13)	−0.011 2(6)	0.284 0(8)	−0.026 4(13)	−0.522 3(13)
C(12)	0.143 3(8)	0.180 5(17)	0.007 9(7)	0.424 2(9)	0.045 2(13)	−0.262 6(14)
O(12)	0.171 8(6)	0.164 9(14)	−0.012 5(6)	0.490 2(8)	0.078 8(11)	−0.280 2(12)
C(13)	0.069 1(7)	0.374 0(15)	0.037 0(7)	0.301 1(8)	0.157 3(13)	−0.167 2(14)
O(13)	0.056 3(4)	0.469 7(11)	0.022 4(5)	0.298 5(6)	0.264 7(11)	−0.138 9(11)
C(21)	0.179 7(7)	0.299 6(16)	0.177 7(7)	0.258 7(8)	−0.173 2(12)	0.082 2(13)
O(21)	0.196 8(5)	0.370 1(11)	0.208 9(5)	0.229 0(6)	−0.173 3(10)	0.186 7(11)
C(22)	0.225 6(7)	0.158 5(16)	0.113 7(7)	0.409 4(9)	−0.171 8(13)	−0.064 0(14)
O(22)	0.264 8(6)	0.155 1(13)	0.095 6(6)	0.471 3(8)	−0.167 6(12)	−0.046 4(12)
C(23)	0.181 9(8)	0.055 3(19)	0.186 1(8)	0.278 7(8)	−0.392 3(14)	−0.133 3(14)
O(23)	0.194 7(6)	−0.013 0(14)	0.215 7(6)	0.261 7(7)	−0.509 1(11)	−0.159 0(12)
C(31)	−0.022 0(9)	0.062 2(19)	0.101 0(8)	0.140 0(9)	−0.228 8(13)	−0.383 1(14)
O(31)	−0.062 7(6)	0.023 3(15)	0.080 8(6)	0.110 9(7)	−0.216 1(11)	−0.463 5(11)
C(32)	0.010 2(9)	0.254 0(19)	0.160 5(8)	0.107 3(10)	−0.253 4(16)	−0.114 1(17)
O(32)	−0.019 4(7)	0.314 6(16)	0.179 4(7)	0.058 3(9)	−0.274 2(14)	−0.031 3(5)
C(33)	0.054 0(9)	0.033 7(20)	0.189 4(9)	0.156 8(10)	−0.438 4(16)	−0.327 2(16)
O(33)	0.058 6(6)	−0.016 7(14)	0.223 3(6)	0.137 7(8)	−0.556 4(12)	−0.377 0(13)
C(1)	0.116 2(6)	0.644 0(14)	0.110 6(6)	0.219 4(7)	0.177 7(12)	0.296 5(12)
C(112)	0.242 1(4)	0.751 2(9)	0.142 5(4)	0.425 1(5)	0.198 7(8)	0.367 0(8)
C(113)	0.289 7(4)	0.791 7(9)	0.171 9(4)	0.470 6(5)	0.229 6(8)	0.473 6(8)
C(114)	0.332 2(4)	0.709 4(9)	0.188 4(4)	0.466 1(5)	0.337 7(8)	0.594 2(8)
C(115)	0.327 1(4)	0.586 5(9)	0.175 6(4)	0.416 2(5)	0.414 9(8)	0.608 3(8)
C(116)	0.279 6(4)	0.545 9(9)	0.146 1(4)	0.370 7(5)	0.384 1(8)	0.501 7(8)
C(111)	0.237 0(4)	0.628 3(9)	0.129 6(4)	0.375 2(5)	0.275 9(8)	0.381 1(8)
C(122)	0.190 4(4)	0.565 2(8)	−0.001 3(5)	0.289 2(5)	0.486 0(8)	0.301 3(8)
C(123)	0.187 0(4)	0.613 2(8)	−0.045 8(5)	0.303 4(5)	0.612 0(8)	0.287 1(8)
C(124)	0.171 4(4)	0.735 1(8)	−0.054 4(5)	0.361 1(5)	0.649 9(8)	0.191 7(8)
C(125)	0.159 5(4)	0.808 9(8)	−0.018 5(5)	0.404 6(5)	0.561 8(8)	0.110 4(8)
C(126)	0.162 9(4)	0.760 9(8)	0.026 0(5)	0.390 4(5)	0.435 8(8)	0.124 5(8)
C(121)	0.178 4(4)	0.639 0(8)	0.034 6(5)	0.332 7(5)	0.397 9(8)	0.220 0(8)
C(212)	0.085 3(3)	0.518 1(8)	0.238 7(4)	−0.007 4(5)	0.014 8(7)	0.207 1(8)
C(213)	0.106 4(3)	0.537 5(8)	0.285 4(4)	−0.073 9(5)	−0.070 9(7)	0.245 7(8)
C(214)	0.148 7(3)	0.622 9(8)	0.298 2(4)	−0.069 5(5)	−0.152 7(7)	0.317 2(8)
C(215)	0.170 0(3)	0.689 0(8)	0.264 4(4)	0.001 4(5)	−0.148 6(7)	0.350 0(8)
C(216)	0.148 9(3)	0.669 7(8)	0.217 7(4)	0.068 0(5)	−0.062 8(7)	0.311 4(8)
C(211)	0.106 6(3)	0.584 2(8)	0.204 8(4)	0.063 6(5)	0.018 9(7)	0.240 0(8)
C(222)	0.000 2(3)	0.726 4(8)	0.162 5(3)	0.140 4(5)	0.318 1(8)	0.074 1(7)
C(223)	−0.050 2(3)	0.789 5(8)	0.152 3(3)	0.123 4(5)	0.436 8(8)	0.087 9(7)
C(224)	−0.091 0(3)	0.750 5(8)	0.116 0(3)	0.087 8(5)	0.505 0(8)	0.211 2(7)
C(225)	−0.081 4(3)	0.648 5(8)	0.089 8(2)	0.069 2(5)	0.454 5(8)	0.320 5(7)
C(226)	−0.031 0(3)	0.585 4(8)	0.100 0(3)	0.086 3(5)	0.335 8(8)	0.306 7(7)
C(221)	0.009 8(3)	0.624 4(8)	0.136 3(3)	0.121 9(5)	0.267 6(8)	0.183 4(7)

reflections were averaged to give 3 556 and 4 666 data with $I > 3.0\sigma(I)$ for (**12**) and (**13**), respectively.

Structure solution and refinement.[24] The positions of the three ruthenium atoms for (**12**) and the two gold atoms for (**13**) were determined from Patterson syntheses. The remaining metal atoms and the other non-hydrogen atoms were located from subsequent difference Fourier syntheses. The phenyl rings were treated as rigid hexagons [d(C–C) = 1.395 Å] and the hydrogen atoms were included in the structure factor calculations at calculated positions [d(C–H) = 1.08 Å] with fixed thermal parameters of 0.08 Å^2. The metal, phosphorus, and sulphur atoms were assigned anisotropic thermal parameters in the final cycles of full-matrix refinement which converged at R and R' values of 0.0641 and 0.0618 for (**12**) and 0.0455 and 0.0461 for (**13**), with weights of $1/\sigma^2(I)$ assigned to individual reflections in both structures. For (**12**) and (**13**), selected bond lengths are given in Table 3 and selected interbond angles in Table 4. The final atomic co-ordinates for both structures are given in Table 5.

Acknowledgements

We thank Drs. M. Murray and V. Šik for their analysis of the $^{31}P\text{-}\{^1H\}$ n.m.r. spectrum of (**9**) and Drs. O. W. Howarth and E. H. Curzon for recording a number of $^{13}C\text{-}\{^1H\}$ and 400-MHz ^1H n.m.r. spectra. In addition, we thank the S.E.R.C. for a studentship (to S. S. D. B.), the Nuffield Foundation for support,

Johnson Matthey Ltd. for a generous loan of gold, silver, and ruthenium salts, Mr R. J. Lovell for technical assistance, and Mrs. L. J. Salter for drawing the diagrams.

References

1 Part 3, M. J. Freeman, A. G. Orpen, and I. D. Salter, *J. Chem. Soc., Dalton Trans.*, 1987, 1001.
2 R. A. Brice, S. C. Pearse, I. D. Salter, and K. Henrick, *J. Chem. Soc., Dalton Trans.*, 1986, 2181.
3 L. J. Farrugia, M. J. Freeman, M. Green, A. G. Orpen, F. G. A. Stone, and I. D. Salter, *J. Organomet. Chem.*, 1983, **249**, 273.
4 M. I. Bruce, O. bin Shawkataly, and B. K. Nicholson, *J. Organomet. Chem.*, 1985, **286**, 427.
5 S. S. D. Brown, I. J. Colquhoun, W. McFarlane, M. Murray, I. D. Salter, and V. Šik, *J. Chem. Soc., Chem. Commun.*, 1986, 53.
6 P. A. Bates, S. S. D. Brown, A. J. Dent, M. B. Hursthouse, G. F. M. Kitchen, A. G. Orpen, I. D. Salter, and V. Šik, *J. Chem. Soc., Chem. Commun.*, 1986, 600.
7 M. J. Freeman, A. G. Orpen, and I. D. Salter, *J. Chem. Soc., Dalton Trans.*, 1987, 379.
8 J. S. Bradley, R. L. Pruett, E. Hill, G. B. Ansell, M. E. Leonowicz, and M. A. Modrick, *Organometallics*, 1982, **1**, 748.
9 S. A. Bezman, M. R. Churchill, J. A. Osborn, and J. Wormald, *J. Am. Chem. Soc.*, 1971, **93**, 2063; D. M. Ho and R. Bau, *Inorg. Chim. Acta*, 1984, **84**, 213.
10 T. H. Lemmen, K. Folting. J. C. Huffman, and K. G. Caulton, *J. Am. Chem. Soc.*, 1985, **107**, 7774.
11 T. Adatia, M. McPartlin, and I. D. Salter, unpublished work.
12 G. B. Ansell, M. A. Modrick, and J. S. Bradley, *Acta Crystallogr., Sect. C*, 1984, **40**, 365.
13 J. A. K. Howard, I. D. Salter, and F. G. A. Stone, *Polyhedron*, 1984, **3**, 567.
14 L. W. Bateman, M. Green, K. A. Mead, R. M. Mills, I. D. Salter, F. G. A. Stone, and P. Woodward, *J. Chem. Soc., Dalton Trans.*, 1983, 2599.
15 B. F. G. Johnson, J. Lewis, W. J. H. Nelson, M. D. Vargas, D. Braga, K. Henrick, and M. McPartlin, *J. Chem. Soc., Dalton Trans.*, 1986, 975.
16 J. A. Iggo, M. J. Mays, P. R. Raithby, and K. Henrick, *J. Chem. Soc., Dalton Trans.*, 1984, 633; B. F. G. Johnson, D. A. Kaner, J. Lewis, P. R. Raithby, and M. J. Taylor, *J. Chem. Soc., Chem. Commun.*, 1982, 314.
17 R. D. Adams and D. A. Katahira, *Organometallics*, 1982, **1**, 53.
18 B-K. Teo and J. C. Calabrese, *Inorg. Chem.*, 1976, **15**, 2474.
19 N. Marsich, A. Camus, and E. Cubulec, *J. Inorg. Nucl. Chem.*, 1972, **34**, 933.
20 H. Schmidbauer, W. Wohlleben, F. Wagner, O. Orama, and G. Huttner, *Chem. Ber.*, 1977, **110**, 1748.
21 G. B. Kauffman and L. A. Teter, *Inorg. Synth.*, 1963, **7**, 9.
22 F. G. Mann, A. F. Wells, and D. Purdie, *J. Chem. Soc.*, 1937, 1828.
23 M. K. Cooper, P. J. Guerney, and M. McPartlin, *J. Chem. Soc., Dalton Trans.*, 1982, 757.
24 G. M. Sheldrick, SHELX 76, program for crystal structure determination, University of Cambridge, 1976.

Received 8*th September* 1986; *Paper* 6/1800